Saliency Detection Based on Non-convex Weighted Surrogates

Yu Yang Min Li* Yao Zhang

Shenzhen Key Laboratory of Advanced Machine Learning and Applications
College of Mathematics and Statistics, Shenzhen University
Shenzhen 518060, Guangdong province, China,
1800201011@email.szu.edu.cn, limin800@szu.edu.cn, jaafar_zhang@163.com

ABSTRACT

Low rank and sparsity decomposition have shown potential for salient object detection. In existing methods, nuclear norm is used to approximate rank minimization and l_1 norm is selected as sparse regularization. Two deficiencies, however, still exist for nuclear norm and l_1 norm. First, both always over-penalize large singular values or large entries of vectors and result in a biased solution. Second, the existing algorithms very slow for large-scale applications. To address these problems, we propose a novel weighted matrix decomposition model with two regularizations: (1) Schatten-2/3 quasi-norm that captures the lower rank of background by matrix factorization technique, and (2) The $l_{2/3}$ - norm that is capable of producing consistent salient object within the same image patches by effectively absorbing both image ge–ometrical structure and feature similarity. In addition, we equip the weighting matrix with a high-level background prior map based on the color, location and boundary connectivity, which can indicate the probability that each image region belongs to the background. The proposed model can be solved by perform SVDs on two much smaller factor matrices. Experiments on three broadly used datasets by detailed comparisons show that our proposed approach has potential in salient object detection.

CCS Concepts

• **Computing methodologies** → **Artificial intelligence** → **Computer vision** → **Computer vision problems** → **Object detection;**

Keywords

Salient object detection; Non-convex weighted matrix decomposition; Low rank and sparsity decomposition;

It is well known that images are one of the main carriers for information transmission. The computer shows ability in detecting and segmenting out important regions of the input image that conforms to the human visual mechanism. This task is called the saliency detection in computer vision, which has been a popular research topic in the past ten years.

In practical approaches, it is worth noting that the deep learning based methods has been a booming research topic for salient object detection in recent years. For example, Liu et al. gave a novel pixel-wise contextual attention network [9]. Hou and Cheng et al. proposed deeply supervised network with short connections [6]. Zhang found progressive attention guided recurrent network with multi-level contextual information [20, 5]. But in this paper, we are interested in another researching branch for saliency detection, i.e. the traditional methods, which aim to build different regularization metrics for salient object and background of an image.

In literature, the most pioneering work was the robust PCA based on low rank matrix recovery (LRMR) [3, 2, 4, 19], in which low rank always is used to formulate the background of an image that lies in a low-dimensional subspace, while sparsity corresponds to the salient object. Since this problem is NP-hard in most cases, many relaxation models and algorithms have been derived. For instance, Shen et al. proposed a unified approach based on low rank matrix recovery (ULR) with low-level feature obtained by high-level guidance [16]. Zou et al. [22] presented an unsupervised model that incorporated bottom-up segmentation (SLR). Peng et al. gave a structured matrix decomposition approach with a tree-structured sparsity regularization (SMD) [13]. Tang et al. proposed a weighted low rank matrix recovery (WLRR) [18].

In these models, the nuclear norm is used to approximate low rank for background information. However, the nuclear norm may lead to the over-penalization for large singular values, which makes solution deviate from the original background. For salient object, l_1 norm is the most common choice for sparsity. But the l_1 norms still over-penalizes large entries of vectors and results in a biased solution [15]. In addition, it is a common assumption for these models that the background should has high contrast with salient object. However, in practice, background has the similar appearance with salient object.

To address these problems, we propose the non-convex surrogates for rank minimization and l_0 norm respectively which can give a closer approximation. In this paper, we consider only Schatten-2/3 norm and $l_{2/3}$ -norm for background and foreground object respectively, since an analytic solution can be derived by using the roots of quartic polynomial in minimization. And a number of experimental results show that Schatten-1/2 norm and $l_{1/2}$ -norm

can give similar results to that of Schatten-2/3 norm and $l_{1/2}$-norm, thus we ignore the 1/2 case due to layout limitation.

In order to completely achieve the separation of salient objects and the background, we propose to adopt the weighting matrix with a high-level background prior map based on the color, location and boundary connectivity, which can indicate the probability that each image area belongs to the background. A flowchart of the proposed model can be illustrated in Figure 1. Particularly, the new model can be seen the extension of WLRR [18] based on non-convex surrogates.

1. PROPOSED MODEL

1.1 Problem Formulation

A given nature image I is over-segmented into N nonoverlapping patches $\mathcal{P} = \{P_1, P_2, \cdots, P_n\}$. For each patch P_i i-th D-dimensional low-level feature vector can be denoted as $f_i \in R^d$. Consequently, a feature matrix of D is formed, which can be written as $D = [f_1, f_2, \cdots, f_n] \in R^{d \times n}$. The problem of salient object detection is to find an efficient model to decompose the feature matrix D into a low-rank part L (background) and a sparse part S (salient object), respectively [13, 18].

To overcome the issues for low-rank and sparsity as introduced in Section 1, we propose a novel weighted bilinear factor matrix norms model for saliency detection as follows:

$$\min_{L,S} \|L\|_{S_{2/3}}^{2/3} + \lambda \|S\|_{l_{2/3}}^{2/3}, \quad \text{s.t.} \quad \text{W} \circ \text{D} = \text{W} \circ L + S. \quad (1)$$

where $\|L\|_{S2/3} = \left(\sum \sigma_k^{2/3}\right)^{3/2}$ ($\sigma_k(L)$ denotes the k-th largest singular value of L) is Schatten-2/3 quasi-norm, $\|S\|_{l_{2/3}} = \left(\sum s_{ij}^{2/3}\right)^{3/2}$ is $l_{2/3}$-norm, W is the weighting matrix and the symbol $\circ$ repre-sents outer product of matrix.

1.2 Schatten-2/3 Quasi-Norm Term For Background

In this section, we first give the Frobenius/nuclear hybrid norm penalty, which has the following equivalence relation with Schatten-2/3 quasi-norm as shown in Definition 1.

Definition 1. [15] For any matrix $X \in R^{m \times n}$ of rank at most $r \leq d$, we decompose it into two factor matrices $U \in R^{m \times d}$ and $V \in R^{n \times d}$ such that $X = UV^T$. Then the Frobenius/nuclear hybrid norm penalty of X is defined as

$$\|X\|_{F-N} = \min_{U,V,X=UV^T} \left(\frac{1}{3}\|U\|_F^2 + \frac{2}{3}\|V\|_*\right)^{3/2}.$$

where $\|\cdot\|_F$ is Frobenius norm of factorization matrix U and $\|\cdot\|_*$ is nuclear norm of factorization matrix V, which avoid the SVD computation on the full matrix X. In fact, the Frobenius/nuclear hybrid norm is a Schatten-2/3 quasi norm, i.e.

$$\|X\|_{S_{2/3}} = \|X\|_{F-N}.$$

And it is noticed that this is different from the weighted nuclear norm, since the solving for the latter is still based on the SVD computation on the full matrix X in spite of the different weight. Compared with nuclear norm (which is in essence the l_q-norm on singular values), the Schatten-2/3 norm is better in capturing the rank function structure. And since norm is factorized, it is only required to perform SVDs on two much smaller factor matrices ($U \in R^{m \times d}$, $V \in R^{n \times d}$) for solving minimization as contrary to the larger ones $X \in R^{m \times n}$ used in the other low-rank based methods. This is particularly useful for many big datasets.

1.3 Weighting Matrix Formulation For Background
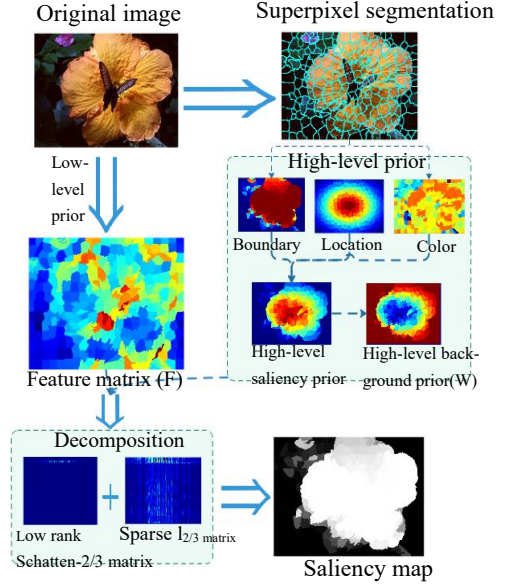
Figure 1. The flowchart illustrations of the proposed model with a weighting background prior, where low rank is characterized by the non-convex Schatten-2/3 quasi-norm and sparsity is approximated by $l_{2/3}$-norm.

The exact depiction of the background is related to color, location and boundary information. It is the common assumption that regions locating near image center are salient in saliency detection. But objects away from the center have a great possibility of being background [8]. On the other hand, the warm color is more conspicuous from the perspective of human visual perception. Thus, color prior is a good background guidance [16]. In addition, it is intuitive that the boundary of image has a great possibility of being part of background [21] and salient objects are almost impossible to relate to boundary. Therefore, inspired by the works in [8, 18, 16, 21], we formulate the weighting matrix integrating color, location and boundary into background.

Location: For each super-pixel P_i, we define the Euclidean distance function $d(p_i, c)$, where p_i denotes the average position, c represents the distance from image center. Then we generate a prior based on the distance via a Gaussian distribution. Thus, Saliency location prior of P_i can be represented as

$$LP(i) = \exp\left(-d(p_i, c) / \sigma_1^2\right) \quad (2)$$

Color: In this section, we continue to adopt the corresponding color prior for each super-pixel P_i as discussed in [16, 18], which denoted as $CP(i)$.

Boundary: According to the length of intersection between a super-pixel P_i and image boundary super-pixels B, we can quantify the possibility of P_i connected to the image boundary. Thus, the boundary connectivity prior of objects is defined as

$$BP(i) = \exp\left(-\frac{|P(i) \cap B|}{N(i)}\right) \quad (3)$$

where $|\cdot|$ denotes the length of intersection, B is the set of boundary super-pixels, and $N(i)$ represents the super-pixel

number of $P(i)$.

Here we fuse the above three priors as a high-level salient prior map as $obj(i)$:

$$obj(i) = LP(i) \cdot CP(i) \cdot BP(i). \tag{4}$$

Then, we recruit $obj(i)$ into the Gauss distribution as an appropriate weight mode, which is

$$W(i) = \exp\left(-\left|obj(i)^2 / \sigma_2^2\right|\right). \tag{5}$$

When the image region belongs to the foreground probability sufficiently small, it will approximate the function property of 1 through (5), which indicates the probability of belonging to the background. Conversely, when the image area belongs to the foreground, it will have a smaller value in the background prior.

Finally, we transfer $W(i)$ to a weighting matrix W as shown in [18]. Obviously, the new weighting matrix is different from one in [18] because of the different location, color, boundary definition and differences in the method of extracting weight matrix.

1.4 Non-convex $l_{2/3}$ Norms For Salient Region

It is well known that a hyper-Laplacian distribution $p(x) \propto e^{k|x|^\alpha}$, $(0.5 \leq \alpha \leq 0.8)$ can be used to characterize the heavy-tailed distribution of sparse outlines and singular values of all channels in low-level vision [15]. Stimulated by this, we propose to employ the non-convex $l_{2/3}$-norm for representing the sparsity of salient object. This norm can not only fully take advantage of the spatial contiguity and feature similarity among image patches, but also find an analytic solution by seeking the roots of a quartic polynomial. Therefore, this regularization has more accurate and consistent representation for salient object.

2. SOLVER OF PROPOSED SALIENCY DETECTION MODEL AND COMPLEXITY ANALYSIS

Motivated by the alternating direction method of multipliers (ADMM) [17], we provide the optimization algorithm for the new model (1). Firstly, replacing $\|\cdot\|_{S2/3}$ by the results of Definition 1, the model (1) can be rewritten as:

$$\min_{U,V,L,S} \frac{1}{3}(\|U\|_F^2 + 2\|V\|_*) + \lambda\|S\|_{2/3}^{2/3} \tag{6}$$
$$\text{s.t.} \quad L = UV^T, \quad W \circ D = W \circ L + S.$$

Then, we need to introduce the auxiliary variable $\widehat{V}$, the problem (6) translates into the following form:

$$\lim_{U,V,L,S,\widehat{V}} \frac{1}{3}(\|U\|_F^2 + 2\|\widehat{V}\|_*) + \lambda\|S\|_{2/3}^{2/3} \tag{7}$$
$$\text{s.t.} \quad L = UV^T, \quad W \circ D = W \circ L + S, \quad \widehat{V} = V.$$

The augmented Lagrangian function for (7) can be given as follows:

$$\begin{aligned}
\mathcal{L}_\mu\left(U,V,L,S,\widehat{V},Y_1,Y_2,Y_3\right) &= \frac{1}{3}\left(\|U\|_F^2 + 2\|\widehat{V}\|_*\right) \\
&+ \lambda\|S\|_{2/3}^{2/3} + \left\langle Y_1, \widehat{V} - V\right\rangle + \left\langle Y_2, UV^T - L\right\rangle \\
&+ \left\langle Y_3, W \circ L + S - W \circ D\right\rangle + \frac{\mu}{2}\left\|\widehat{V} - V\right\|_F^2 \\
&+ \left\|UV^T - L\right\|_F^2 + \left\|W \circ L + S - W \circ D\right\|_F^2)
\end{aligned} \tag{8}$$

where Y_1, Y_2, Y_3 are the introduced Lagrange multipliers, $\langle \cdot, \cdot \rangle$ is the inner product of the matrix and μ is penalty coefficient.

2.1 Updating U_{k+1} and V_{k+1}

To update U_{k+1} and V_{k+1}, we consider the following optimization problems:

$$\min_U \frac{1}{3}\|U\|_F^2 + \frac{\mu_k}{2}\left\|\mu_k^{-1}Y_2^k + UV_k^T - L_k\right\|_F^2, \tag{9}$$

$$\min_V \left\|\mu_k^{-1}Y_1^k + \widehat{V}_k - V\right\|_F^2 + \left\|\mu_k^{-1}Y_2^k + U_{k+1}V^T - L_k\right\|_F^2. \tag{10}$$

Since (9) and (10) are least squares problems, the optimal soluteions can be represented as:

$$U_{k+1} = \mu_k(L_k - \mu_k^{-1}Y_2^k)V_k\left(\frac{2}{3}I + \mu_k V_k^T V_k\right)^{-1}, \tag{11}$$

$$V_{k+1} = \left(\widehat{V}_k + \mu_k^{-1}Y_1^k + \left(L_k - \mu_k^{-1}Y_2^k\right)^T U_{k+1}\right)\left(I + U_{k+1}^T U_{k+1}\right)^{-1} \tag{12}$$

2.2 Updating $\widehat{V}_{k+1}$

To solve $\widehat{V}_{k+1}$, we fix the other variables and solve the following optimization problem:

$$\min_{\widehat{V}} \frac{2}{3\mu_k}\|\widehat{V}\|_* + \frac{1}{2}\left(\left\|\widehat{V} - \left(V_{k+1} - \mu_k^{-1}Y_1^k\right)\right\|_F^2\right) \tag{13}$$

The minimization (13) is a regularized least squares problem associated with the nuclear norm, of which closed-form solution can be represented by the singular value thresholding (SVT) [2] (refers Theorem 1).

Theorem 1 (SVT [2]). Let the singular value decomposition of C can be written as $C = U\Sigma V^T$, then the optimal solution for B is given by

$$B = \mathcal{D}_\varepsilon(C) = U\mathcal{S}_\varepsilon V^T, \tag{14}$$

where $\mathcal{D}_\varepsilon$ is the singular value thresholding operator and $\mathcal{D}_\varepsilon$ which is defined as

$$\mathcal{S}_\varepsilon = \begin{cases} x - \mathcal{E} & x > \mathcal{E} \\ 0 & otherwise \end{cases}. \tag{15}$$

2.3 Updating L_{k+1}

Fixing other variable, L_{k+1} can be updated by the following problem:

$$\min_L \left\|\mu_k^{-1}Y_2^k + U_{k+1}V_{k+1}^T - L\right\|_F^2 + \left\|\mu_k^{-1}Y_3^k + W \circ L + S_k - W \circ D\right\|_F^2. \tag{16}$$

Thus, the solution of problem (16) is given as

$$\begin{aligned}
L + L \circ W \circ W &= \mu_k^{-1}Y_2^k + U_{k+1}V_{k+1}^T - \mu_k^{-1}Y_3^k \circ W \\
&+ W \circ D \circ W - W \circ S_k.
\end{aligned} \tag{17}$$
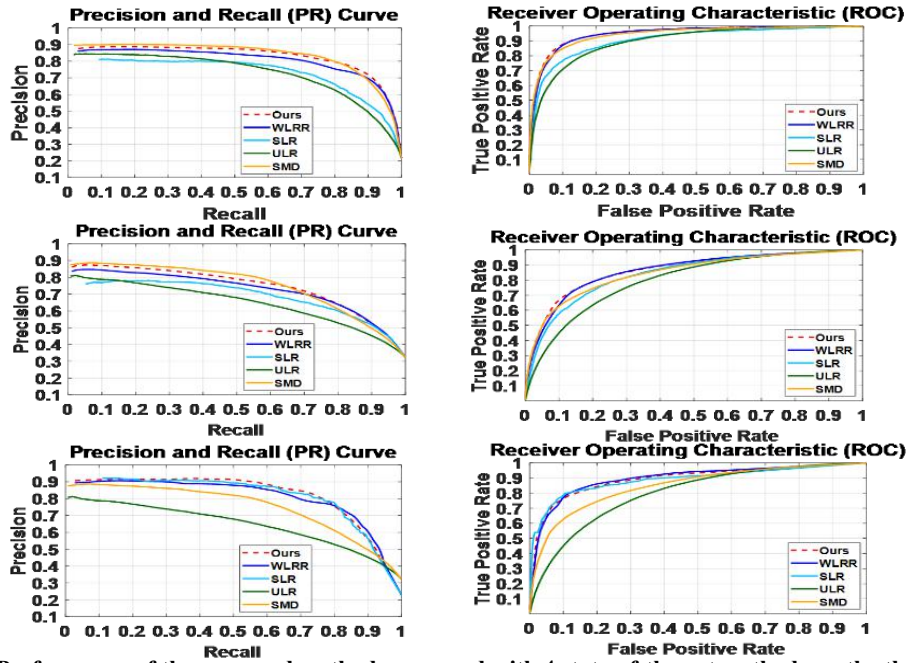
Figure 2. Performance of the proposed method compared with 4 state-of-the-art methods on the three datasets: iCoSeg [7], PASCAL-S[11] and SED2[1].

2.4 Updating S_{k+1}

Fixing other variables, updating of S_{k+1} can be summarized as the following sub-problem.

$$\arg\min_{S} \frac{1}{2}\|S-G\|_F^2 + \frac{\lambda}{\mu_k}\|S\|_{l_{2/3}}^{2/3} \qquad (18)$$

where $G = W \circ D - W \circ L_{k+1} - \mu_k^{-1}Y_3^k$ .Therefore, the problem (18) can be solved by Theorem 2.

Theorem 2. [15] For any matrix $S \in R^{m \times n}$, solution of the following minimization

$$\min_{S}\|S-C\|_F^2 + \gamma\|S\|_{l_{2/3}}^{2/3} \qquad (19)$$

is $S^* = \mathcal{T}_\gamma(C)$.

where the 2/3-thresholding operator $\mathcal{T}_\gamma(C)$ is

$$\mathcal{T}_\gamma(c_{ij}) = \begin{cases} \dfrac{\text{sign}(c_{ij})\left(\psi_\gamma(c_{ij})+T\right)^3}{8} & |c_{ij}| > w \\ 0 & otherwise \end{cases} \qquad (20)$$

where

$$\psi_\gamma(c_{ij}) = \frac{2}{\sqrt{3}}\sqrt{\sqrt{\gamma}\cosh\left(\frac{\text{arccosh}\left(\frac{27c_{ij}^2}{16}\gamma^{-3/2}\right)}{3}\right)}, \; w = \frac{2\sqrt[4]{3r^3}}{3}, \; T = \sqrt{\frac{2|c_{ij}|}{\psi_\gamma(c_{ij})} - \psi_\gamma^2(c_{ij})}.$$

Finally, the Lagrange multipliers $Y_i, (i=1,2,3)$ and penalty parameter μ can be represented as follows:

$$Y_1^{k+1} = Y_1^k + \mu_k\left(\widehat{V}_{k+1} - V_{k+1}\right), \qquad (21)$$

$$Y_2^{k+1} = Y_2^k + \mu_k\left(U_{k+1}V_{k+1}^T - L_{k+1}\right), \qquad (22)$$

$$Y_3^{k+1} = Y_3^k + \mu_k\left(S_{k+1} + W \circ L_{k+1} - W \circ D\right), \qquad (23)$$

$$\mu_{k+1} = \min(\rho\mu_k, \mu_{max}). \qquad (24)$$

2.5 Complexity analysis

The per-iteration cost of existing low-rank based methods, such as WLRR [18], SMD [13], ULR [16] and SLR [22], are dominated by the computation of the thin SVD for an $m \times n$ matrix with $m \geq n$, and is $O(mn^2)$. The cost of computing the inverse for $d \times d$ matrix is $O(d^3)$, and the expense of multiplication for $m \times d$ matrix and $d \times n$ matrix is $O(mdn)$. But for the proposed model (1), the dominant cost of each iteration for updating $U \in R^{m \times d}$, $V \in R^{n \times d}$ and $\widehat{V} \in R^{n \times d}$ using Eq.11, Eq.12 and Eq.14 is $O(6mnd + 2d^3 + md^2 + nd^2)$. Therefore, we deduce that $O(6mnd + 2d^3 + md^2 + nd^2) \ll O(mn^2)$ for $m, n \gg d$.

3. EXPERIMENT

We use three standard benchmark datasets such as iCoSeg[7], PASCAL-S[11] and SED2[1] to represent different scenarios. The iCoSeg dataset includes images with multiple objects, various size and location, while the PASCAL-S dataset involves total 850 images with various objects and complex backgrounds. The SED2 dataset is used to evaluate performance on images containing two salient objects.

In order to assess experimental results, we adopt seven common evaluation metrics used in salient object detection. For example, Receiver Operating Characteristic (ROC) [13], Precision and Recall (PR) [13], F-measure curve[13, 10] Weighted F-measure (WF)[12], Overlap Ratio (OR)[10], Area Under Curve (AUC) and Mean Absolute Error (MAE)[14].

Table 1 reports the comparison of new model and the other low rank approaches, such as SLR[22], WLRR[18], SMD[13] and ULR [16]. On iCoSeg[7], our model gives the best metric results in terms of WF, OR and MAE and the second best in AUC. On PASCAL-S[11], OR, MAE and AUC from our model are obviously the best, and the WF is the second best. For SED2[1], the new model also represents more potential results in WF, OR and MAE.

Table 1. Comparison results with low-rank models and performance boost with different baselines on Datasets. The best two results are highlighted with red, blue fonts, respectively.

iCoSeg [7]	evaluate	our model	SLR [22]	WLRR [18]	SMD [13]	ULR [16]
	WF ↑	0.618	0.473	0.602	0.611	0.379
	OR ↑	0.608	0.505	0.578	0.598	0.443
	AUC ↑	0.842	0.805	0.843	0.822	0.814
	MAE ↓	0.137	0.179	0.147	0.137	0.222
PASCAL-S[11]	WF ↑	0.514	0.398	0.535	0.485	0.320
	OR ↑	0.458	0.390	0.434	0.444	0.351
	AUC ↑	0.747	0.711	0.746	0.730	0.718
	MAE ↓	0.245	0.275	0.254	0.246	0.295
SED2[1]	WF ↑	0.642	0.565	0.632	0.636	0.385
	OR ↑	0.597	0.560	0.575	0.588	0.428
	AUC ↑	0.793	0.804	0.800	0.776	0.799
	MAE ↓	0.146	0.169	0.157	0.142	0.238

Figure 2 shows the PR and ROC curves comparisons respectively on three datasets. Note that the proposed model has significantly better performance than the other low-rank methods. And Figure 3 give some quantitative visual results based on the four state-of-the-art models. It is easy to find that our model is able to detect complete and consistent salient objects from complex background.

4. CONCLUSION

In this paper, a new weighted model by using Schatten-2/3 norm and $l_{2/3}$ norm for conducting the salient object detection is presented, aiming at the improvement of both accuracy and efficiency of the problem. Compared with low-rank based methods, the non-convex Schatten-2/3 norm can capture the low-rank structure of the background details. The non-convex $l_{2/3}$ norm has ability in characterizing the sparsity of salient object, and can share the consistency within the same image patches. The corresponding optimization process is only required to handle two small size matrices by an appropriate matrix factorization, which simplifies the approach. Experiments on the iCoSeg PASCAL-S and SED2 datasets show that the proposed model has potential in saliency detection.

5. ACKNOWLEDGMENTS

6. REFERENCES

[1] A. Borji, M.-M. Cheng, H. Jiang, and J. Li. Salient object detection: A benchmark. IEEE *transactions on image processing*, 24(12):5706–5722, 2015.

[2] J.-F. Cai, E. J. Cand`es, and Z. Shen. A singular value thresholding algorithm for matrix completion. *SIAM Journal on Optimization*, 20(4):1956–1982, 2010.

[3] E. Cand`es and B. Recht. Exact matrix completion via convex optimization. *Foundations of Computational Mathematics*, 9:717–772, 2009.

[4] V. Chandrasekaran, S. Sanghavi, P. A. Parrilo, and A. S. Willsky. Rank-sparsity incoherence for matrix decomposition. *SIAM Journal on Optimization*, 21(2):572–596, 2011.

[5] Y. Han, C. Xu, G. Baciu, M. Li, and M. R. Islam. Cartoon and texture decomposition-based color transfer for fabric images. *IEEE Transaction on Multimedia*, 19(1):80–92, 2017.

[6] Q. Hou, M. Cheng, X. Hu, A. Borji, Z. Tu, and P. H. S. Torr. Deeply supervised salient object detection with short connections. pages 1–14, 2018.

[7] Y. Jia and M. Han. Category-independent object-level saliency detection. In *Proceedings of the IEEE international conference on computer vision*, pages 1761–1768, 2013.

[8] T. Judd, K. Ehinger, F. Durand, and A. Torralba. Learning to predict where humans look. In *2009 IEEE 12th international conference on computer vision*, pages 2106–2113. IEEE, 2009.

[9] N. Li, J. Han, and M. Yang. Picanet: Learning pixel-wise contextual attention for saliency detection. In 2018 IEEE Conference on Computer Vision and Pattern Recognition, pages 3089–3098, 2018.

[10] X. Li, Y. Li, C. Shen, A. Dick, and A. Van Den Hengel. Contextual hypergraph modeling for salient object detection. In *Proceedings of the IEEE international conference on computer vision*, pages 3328–3335, 2013.

[11] Y. Li, X. Hou, C. Koch, J. M. Rehg, and A. L. Yuille. The secrets of salient object segmentation. In *Proceedings of the IEEE Conference on Computer Vision and Pattern Recognition*, pages 280–287, 2014.

[12] R. Margolin, L. Zelnik-Manor, and A. Tal. How to evaluate foreground maps? In *Proceedings of the IEEE conference on computer vision and pattern recognition*, pages 248–255, 2014.

[13] H. Peng, B. Li, H. Ling, W. Hu, W. Xiong, and S. J. Maybank. Salient object detection via structured matrix decomposition. *IEEE transactions on pattern analysis and machine intelligence*, 39(4):818–832, 2017.

[14] F. Perazzi, P. Kr¨ahenb¨uhl, Y. Pritch, and A. Hornung. Saliency filters: Contrast based filtering for salient region detection. In *2012 IEEE conference on computer vision and pattern recognition*, pages 733–740. IEEE, 2012.

[15] F. Shang, J. Cheng, Y. Liu, Z.-Q. Luo, and Z. Lin. Bilinear factor matrix norm minimization for robust pca: Algorithms and applications. *IEEE transactions on pattern analysis and machine intelligence*, 40(9):2066–2080, 2018.

[16] X. Shen and Y. Wu. A unified approach to salient object detection via low rank matrix recovery. In *2012 IEEE Conference on Computer Vision and Pattern Recognition*, pages 853–860. IEEE, 2012.

[17] Y. Shen, Z. Wen, and Y. Zhang. Augmented lagrangian alternating direction method for matrix separation based on low-rank factorization. *Optimization Methods and Software*, 29(2):239–263, 2014.

---

* Corresponding author.

| Img | ULR[16] | SLR[22] | WLRR[18] | SMD[33] | Ours | GT |
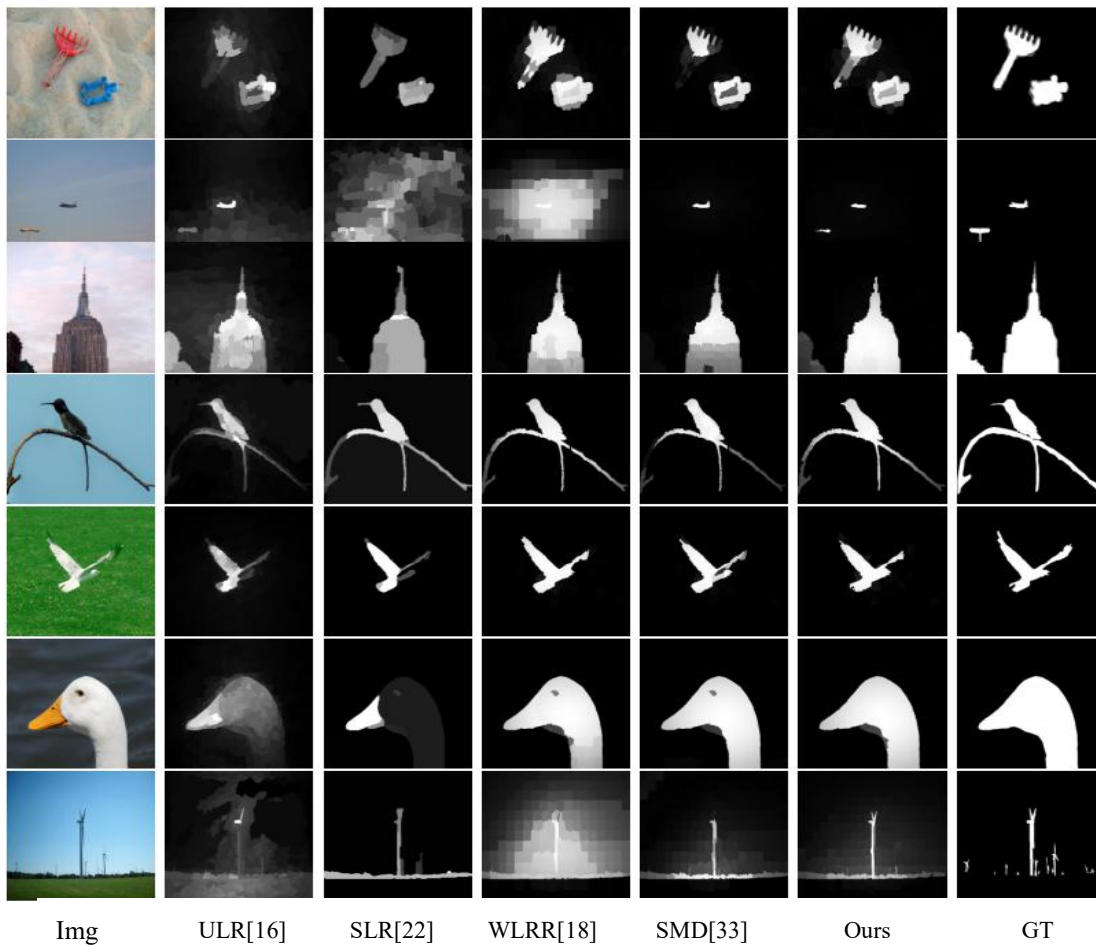
Figure 3. Visual comparison of saliency maps of some state-of-the-art methods on different dataset.

[18] C. Tang, P. Wang, C. Zhang, and W. Li. Salient object detection via weighted low rank matrix recovery. *IEEE Signal Processing Letters*, 24(4):490–494, 2017.

[19] J. Wright, A. Ganesh, S. Rao, Y. Peng, and Y. Ma. Robust principal component analysis: Exact recovery of corrupted low-rank matrices via convex optimization. In *Advances in neural information processing systems*, pages 2080–2088, 2009.

[20] X. Zhang, T. Wang, J. Qi, H. Lu, and G. Wang. Progressive attention guided recurrent network for salient object detection. In *2018 IEEE Conference on Computer Vision and Pattern Recognition*, pages 1–9, 2018.

[21] W. Zhu, S. Liang, Y. Wei, and J. Sun. Saliency optimization from robust background detection. In *Proceedings of the IEEE conference on computer vision and pattern recognition*, pages 2814–2821, 2014.

[22] W. Zou, K. Kpalma, Z. Liu, and J. Ronsin. Segmentation driven low-rank matrix recovery for saliency detection. In *24th British machine vision conference (BMVC)*, pages 1–13, 2013.